journal of the mechanical behavior of biomedical materials 160 (2024) 106756

Contents lists available at ScienceDirect

Journal of the Mechanical Behavior of Biomedical Materials

journal homepage: www.elsevier.com/locate/jmbbm

Influence of silver coated zeolite fillers on the chemical and mechanical properties of 3D-printed polyphenylene sulfone restorations

Felicitas Mayinger [a,*], Andrea Lösch [b,1], Elena Reznikova [c], Christian Wilhelm [b], Bogna Stawarczyk [a]

[a] Department of Prosthetic Dentistry, University Hospital, LMU Munich, Goethestraße 70, 80336, Munich, Germany
[b] Department of Chemistry – Technical Chemistry, RPTU Kaiserslautern-Landau, Erwin-Schrödinger-Straße 54, 67663, Kaiserslautern, Germany
[c] Apium Additive Technologies GmbH, Siemensallee 84, 76187, Karlsruhe, Germany

ARTICLE INFO

Keywords:
Polyphenylene sulfone
Antimicrobial fillers
3D-printing
Chemical properties
Mechanical properties

ABSTRACT

Objectives: To investigate the chemical and mechanical properties of polyphenylene sulfone (PPSU) depending on its composition and manufacturing.
Methods: Unfilled–PPSU1 and with antimicrobial silver coated zeolites filled–PPSU2 specimens were made of granulate–GR, filament–FI, or printed–3D. Scanning microscopy and X-ray spectroscopy were performed. Martens hardness–HM, elastic indentation modulus–E_{IT} and flexural strength–FS were determined initially and after aging. Shear bond strength–SBS to veneering and luting composite after conditioning with 7 adhesive systems were examined after aging. Silver leaching was tested after 1-, 3-, 7-, 14-, 21-, 28- and 42 days. Analyses of variance, Kolmogorov–Smirnov, Kruskal–Wallis, Mann–Whitney *U*, unpaired t-tests and Weibull modulus were computed ($p < 0.05$).
Results: Zeolites were homogeneously distributed. PPSU1-GR and PPSU1-FI showed the highest HM/E_{IT}, followed by PPSU2-GR, PPSU1-3D and PPSU2-3D. PPSU2-FI presented the lowest HM/E_{IT}, displaying micro pits. Aging showed reduced HM/E_{IT} in PPSU1 and no impact on PPSU2, while FS increased (PPSU1) or decreased (PPSU2). PPSU2-3D presented lower FS than PPSU1-3D. High SBS to the luting (7.0–16.2 MPa) and veneering composite (11.8–22.2 MPa), except for adhesive system PR, were observed. PPSU2-3D showed the highest silver release (9.6%), with all compositions dispensing silver over 42 days.
Conclusions: For the examined period of 6 weeks, antimicrobial silver ions were released from filled PPSU. The high SBS between PPSU and veneering/luting composite confirmed the feasibility of esthetically veneering and luting filled PPSU. To achieve mechanical properties like unfilled PPSU, the processing parameters of filled PPSU require refinement.
Clinical significance: This investigation provides proof of principle that PPSU can be successfully doped with silver-coated zeolites. The combination of 3D-printing with an antimicrobial thermoplastic constitutes a great opportunity in the field of prosthetic dentistry. Potential applications include clasps for removable dental prostheses, provisional or permanent fixed dental prostheses and implant abutments.

1. Introduction

Polyphenylene sulfone (PPSU) is a thermoplastic that is new to dentistry. First investigations have reported promising findings for the mechanical properties of this material (Schonhoff et al., 2021, 2022) that underscore its potential in the manufacturing of both removable and fixed dental prostheses (FDPs). Surface pretreatments devised for the tried and tested polyetheretherketone (PEEK) could be successfully transferred to PPSU to ensure the requisite adhesion to other dental materials (Schonhoff et al., 2022). These fundamental advances paved the way for the successful veneering of PPSU restorations that guarantee a high-end esthetic outcome (Mayinger et al., 2023).

One key characteristic that has spurred research endeavors is the potential to process PPSU by three-dimensional (3D) -printing. In

* Corresponding author. Department of Prosthetic Dentistry University Hospital, LMU, Munich, Goethestrasse 70, 80336, Munich, Germany.
E-mail address: felicitas.mayinger@med.uni-muenchen.de (F. Mayinger).
[1] Both authors contributed equally.

https://doi.org/10.1016/j.jmbbm.2024.106756
Received 25 July 2024; Received in revised form 11 September 2024; Accepted 25 September 2024
Available online 26 September 2024

comparison to methyl methacrylate-based resins that are shadowed by their residual monomer content, PPSU is defined by a high biocompatibility (Wenz et al., 1990). With PPSU only existing in an amorphous state (Dorf et al., 2018) and thus being independent of the elaborate fine-tuning of the thermal processing conditions that is indispensable for semi-crystalline materials such as PEEK (Yang et al., 2017), the properties of 3D-printed restorations made from PPSU may be more predictable. To fabricate a 3D-printed object from PPSU, the base material must be processed in two steps. Firstly, granulate is extruded into filament in an operation that requires a strict adherence to the temperature settings and a previously carefully dried material. Secondly, the filament is processed by fused filament fabrication (FFF), where it is carefully heated and extruded to form a 3D structure layer by layer. In this context, the employed printing parameters are decisive (Li and Lou, 2020; Prechtel et al., 2020; Wickramasinghe et al., 2020; Liaw et al., 2021; Wang et al., 2021; Fountas et al., 2022; Kechagias, 2024; Naveed and Anwar, 2024). The interactions between the temperature of the printing bed, the printing chamber and the printing nozzle as well as the printing speed and layer thickness have to be carefully coordinated to ensure cohesion between the different layers and a high precision of the printed object (Wickramasinghe et al., 2020). At the same time, some economic efficiency, that will in the future translate into minimum waiting periods on part of the dental technician, dentist and patient, need to be incorporated.

Recent efforts have focused on altering the composition of PPSU to attain an antimicrobial effect that reduces the attachment of dental plaque. For this purpose, PPSU can be doped with silver containing zeolite fillers. Silver has been known as an antimicrobial agent for centuries and is successfully used in many different applications, from medical devices to cosmetics (Chernousova and Epple, 2013). The zeolite, which consists of microporous aluminosilicates composed of $SiO_{4/2}$- and $AlO_{4/2}$- tetrahedra, is employed as a supporting material to enable the doped PPSU to release antimicrobial silver over a period of time.

The intended application as a dental restorative material calls for PPSU to exhibit sufficient surface properties, a high mechanical strength as well as a successful adhesion to other dental materials. To successfully operate as a bioactive material, PPSU should emit antimicrobial substances over a prolonged duration. SEM and EDX analyses can be employed for a qualitative surface characterization. The determination of PPSU's Martens parameters can be considered for a quantitative surface characterization. The examination of flexural strength (FS) enables the assessment of PPSU's mechanical performance, while the determination of the shear bond strength (SBS) to a veneering and luting resin composite allows deductions on the success of veneering or luting PPSU restorations. The investigation of its leaching properties can determine its antimicrobial behavior, since this property is often related to the amount of silver released from the material (Boschetto et al., 2012; Kuroki et al., 2010; Malic et al., 2019; Stencel et al., 2018; Yamamoto et al., 1996). To allow a close approximation of the in-vitro test set-ups to the clinical situation, adequate aging simulations were included.

The aim of this investigation was to determine the chemical and mechanical properties of PPSU depending on its composition (unfilled or filled with silver coated zeolites) and as a function of its manufacturing process by examining granulate, filament and 3D-printed objects. The following null hypotheses were investigated: (1) the material composition would not show an impact of the surface characteristics of PPSU, (2) neither the material composition nor (3) aging would show an impact on the Martens parameters and FS, (4) the adhesive systems would not influence the SBS to a veneering or luting resin composite, and (5) neither the material composition nor (6) the progression of release time of the silver ions would present an influence on the leaching properties of PPSU.

2. Material and methods

Unfilled (PPSU1) and filled (PPSU2) polyphenylene sulfone (Gehr, Mannheim, Germany) specimens were made of granulate (GR), cut from filament (FI), or fabricated by 3D-printing (3D) (Table 1). Scanning microscope (SEM) images and energy dispersive X-ray spectroscopy (EDX) mappings were performed. The Martens parameters, Martens hardness (HM) and elastic indentation modulus (E_{IT}), and FS were determined initially and after aging (Fig. 1).

SBS to a veneering and luting resin composite after aging were examined as a function of the employed adhesive system. Silver leaching was tested after 1-, 3-, 7-, 14-, 21-, 28- and 42 days.

2.1. Specimen preparation

For SEM/EDX imaging and HM/E_{IT} measurements, all six material variations (PPSU1-GR, PPSU1-FI, PPSU1-3D, PPSU2-GR, PPSU2-FI, PPSU2-3D, N = 120, n = 20/group) were examined. FS was determined for PPSU1-3D and PPSU2-3D (N = 160, n = 20/group). SBS to a veneering and luting resin composite was investigated for PPSU2-3D (N = 70, n = 5/group). Filled specimens (PPSU2-GR, PPSU2-FI and PPSU2-3D) were investigated for silver leaching (N = 3, n = 1/group).

Zeolite was purchased from Zeolyst International (CBV 2314, Conshohocken, USA) and modified to contain 9.9 wt% silver. Unfilled PPSU was doped with 8 wt% of these silver containing zeolite fillers to fabricate filled PPSU. Specimens were made of granulate (GR), cut from filament (FI, n = 40) or printed (3D, n = 270) using filament (Fig. 2).

3D-printed specimens were manufactured (Apium P155, Apium Additive Technologies GmbH, Karlsruhe, Germany (PPSU1) or Apium P220, Apium Additive Technologies GmbH (PPSU2)) with a dimension of 2 × 3 × 15 mm (XY-plane: 3 × 15, Z building height: 2 mm) using a stainless-steel nozzle with a 0.4 mm bore heated to a temperature of 410 °C. The build space was heated to 150 °C. During the printing process, a zone heater tempered to 160 °C (PPSU1) or 150 °C (PPSU2) (Apium Adaptive Heating System, Apium Additive Technologies GmbH) directly transferred heat to the specimens. Printing was performed in 0.15 mm thick layers at a speed of 400 mm/min (PPSU1) or 600 mm/min (PPSU2).

For HM/E_{IT} and SBS measurements, granulate, filament and 3D-printed specimens were embedded in acrylic embedding resin (ScanDiQuick A, and B, ScanDia, Hagen, Germany). All specimens except for PPSU2-GR and PPSU2-FI designated for the investigation of their leaching behavior were polished up to grain P1200 (SiC-paper, Ø 200 mm, Struers, Ballerup Sogn, Denmark) under water cooling with an automatic grinding and polishing machine (Tegramin 20, Struers), and cleaned for 5 min in distilled water using an ultrasonic bath (Sonorex, BANDELIN electronic, Berlin, Germany).

Specimens designated for SBS measurement were air-particle abraded with aluminum-oxide (Al_2O_3) particles with a particle size of 110 μm employing a pressure of 0.2 MPa (basis Quattro IS, Renfert, Hilzingen, Germany) at an angle of 45° with a spacing of 10 mm, subsequently cleaned for 1 min in distilled water in an ultrasonic bath (Sonorex, BANDELIN electronic) and dried with compressed air. Surface conditioning was performed with 7 different adhesive systems (n = 10/subgroup) according to the manufacturers' instructions of use (Table 1). Immediately afterwards, a PMMA cylinder (SD Mechatronik, Feldkirchen-Westerham, Germany) was placed on the specimen surface and filled with a veneering (n = 5/subgroup; crea. lign, bredent, Senden, Germany) or a luting resin composite (n = 5/subgroup; DuoCem, Coltène Whaledent, Altstätten, Switzerland). Each cylinder had an internal diameter of 2.9 mm and a height of 10 mm. Subsequent to polymerization, all specimens were stored dry for 24 h.

2.2. Artificial aging

HM and E_{IT} were examined longitudinally in the initial state and

Table 1
Materials, abbreviations, manufacturers, compositions, Lot.No. and manufacturers' instructions used.

Material	Abbreviation	Manufacturer	Composition	Lot.No.	Manufacturer's instruction for use		
					massage in [s]	blow off [s]	polymerize [s]
unfilled PPSU granulate	PPSU1-GR	Gehr, Mannheim, Germany	PPSU	N/A	–	–	–
unfilled PPSU filament	PPSU1-FI			N/A	–	–	–
unfilled PPSU 3D-printed	PPSU1-3D			N/A	–	–	–
filled PPSU granulate	PPSU2-GR		PPSU, 8 wt% zeolite fillers containing 9.9 wt% silver	N/A	–	–	–
filled PPSU filament	PPSU2-FI			N/A	–	–	–
filled PPSU 3D-printed	PPSU2-3D			N/A	–	–	–
Adhese Universal	AD	Ivoclar Vivadent, Schaan, Liechtenstein	Hydroxyethylmethacrylate, bisphenol A-glycidyl methacrylate, ethanol, 1,10-decandiol dimethylacetamide, methacrylated phosphoric acid ester, camphorquinone, 2-(Dimethylamino)ethyl methacrylate	Y26226	20	until glossy	10[a]
CLEARFIL Universal Bond Quick	CQ	Kuraray, Tokyo, Japan	Bisphenol A-glycidyl methacrylate, ethanol, hydroxyethylmethacrylate	000036	10	5	10[a]
One Coat 7 Universal	OC	Coltène/ Whaledent, Altstätten, Switzerland	Ethanol, urethane dimethacrylate, hydroxyethylmethacrylate	J41100	20	5	10[a]
Peak Universal Bond	PB	Ultradent, Köln, Germany	Ethanol, hydroxyethylmethacrylate, organophosphine oxide, butylated hydroxytoluene, chlorhexidine	BHDBK	10	10	10[a]
Prime&Bond active	PR	Dentsply Sirona, Konstanz, Germany	Bisacrylamide 1, propan-2-ol, 10-Methacryloyloxy-decyl dihydrogen phosphate, dipentaerythritol pentaacrylate phosphate, camphorquinone, 4-dimethylaminobenzonitrile	1,811,004,258	20	5	10[a]
Scotchbond Universal	SB	3M, Seefeld, Germany	Hydroxyethylmethacrylate, bisphenol A-glycidyl methacrylate, silane treated silica, decamethylene dimethylacetamide, water, ethanol, methacrylic phosphoric acid, copolymer of acrylic and itaconic acid, camphorquinone, 1,2-dibromoethane, dimethylaminoethyl acrylate, butanone	4181541	20	5	10[a]
visio.link	VL	bredent, Senden, Germany	Methyl methacrylate, 2-propenoic acid, bisphenol A-glycidyl methacrylate, diphenyl (2,4,6-trimethylbenzoyl) phosphine oxide	193211	Yes, duration not specified	Yes, duration not specified	90[b]
crea.lign	–	bredent, Senden, Germany	Acrylate resins, inorganic fillers, initiators, pigments	123765	–	–	360[b]
DuoCem	–	Coltène Whaledent, Altstätten, Switzerland	10 – < 15% bisphenol A-glycidyl methacrylate, 5 – < 10% triethylene glycol dimethacrylate, 1 – < 5% coated zinc oxide, <1% dibenzoyl peroxide, benzoyl peroxide, <1% sodium fluoride	J49767	–	–	180[c]

[a] Polymerized using Elipar S10, 3M.
[b] Polymerized using bre-lux power unit, bredent.
[c] Polymerized using Labolight DUO, GC Europe.

after aging with 5000 thermal cycles (TC), 10,000 TC, 10,000 TC plus 36 days dry storage and 10,000 TC and 36 days dry storage plus 10,000 TC. FS was determined initially, after 5000 TC and after 10,000 TC. All SBS specimens underwent artificial aging with 10,000 TC. Thermocycling was performed in 5 °C and 55 °C tempered distilled water, with HM/E_{IT} and FS specimens remaining in each bath for 20 s (Technical Committee ISO/TC 106/SC 1, 2015) and SBS specimens remaining in each bath for 30 s (Technical Committee ISO, 2011) (Thermocycler THE-1100, SD Mechatronik). Prior to the different measurements, all specimens were stored dry at room temperature for 1 h.

Silver leaching was measured after 1-, 3-, 7-, 14-, 21-, 28- and 42 days.

2.3. SEM and EDX measurements

Qualitative surface characterization was performed using a scanning electron microscope (JSM-6490LA, JEOL, Freising, Germany). For the granulate and filament, the outer surface was examined. For 3D-printed specimens, the XY-plane was investigated. The specimens were sputter-coated with gold (JFC-1200 Fine Coater, JEOL) for 30 s and SEM images and EDX mappings were made at a x150 magnification at 15 kV with a working distance of 10 mm. Silicon was chosen for EDX mapping as it is the main component of the zeolite and therefore the most detectable.

2.4. Martens parameters measurement

HM [N/mm^2] and E_{IT} [kN/mm^2] were determined with a universal hardness testing machine (ZHU 0.2/Z2.5, ZwickRoell, Ulm, Germany) by pressing a Vickers diamond indenter ($\alpha = 136^\circ$) vertically into the specimen surface with a maximum force of 9.807 N for 20 s (Fig. 3). HM and E_{IT} were calculated (Technical Committee ISO/TC 164/SC 3, 2022) and force-displacement diagrams recorded (testX-pert V12.3 Master,

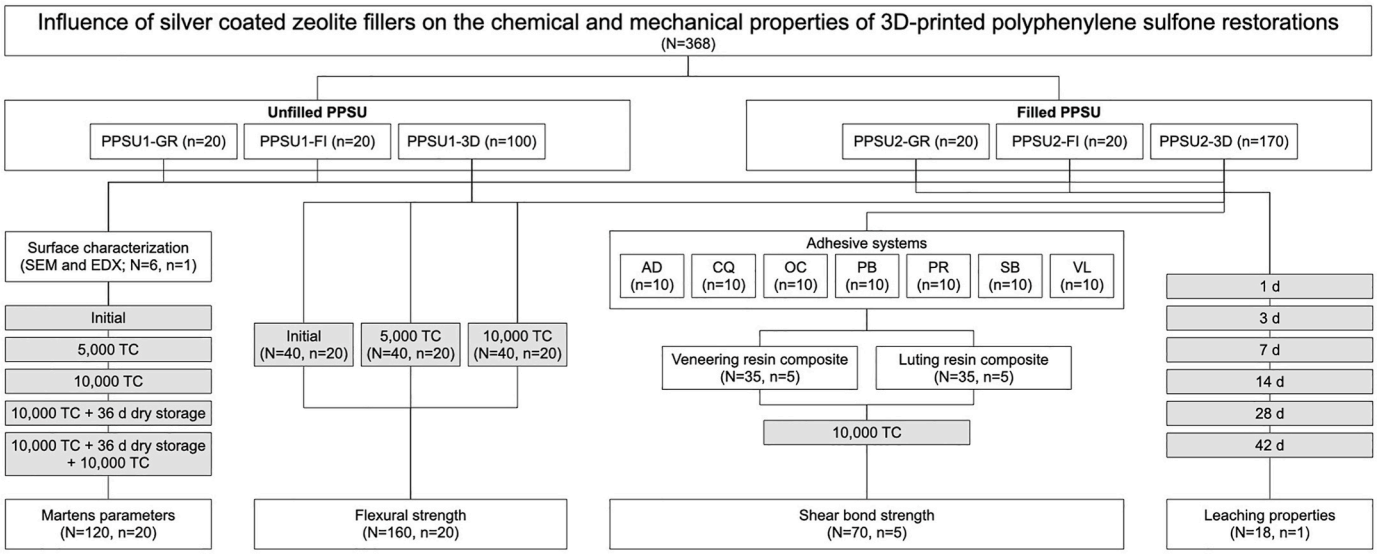

Fig. 1. Study Design (PPSU1 – unfilled, PPSU2 – filled; GR – granulate, FI – filament, 3D – 3D-printed; TC – thermocycles; AD - Adhese Universal, CQ - CLEARFIL Universal Bond Quick, OC - One Coat 7 Universal, PB - Peak Universal Bond, PR - Prime&Bond active, SB - Scotchbond Universal, VL – visio. link).

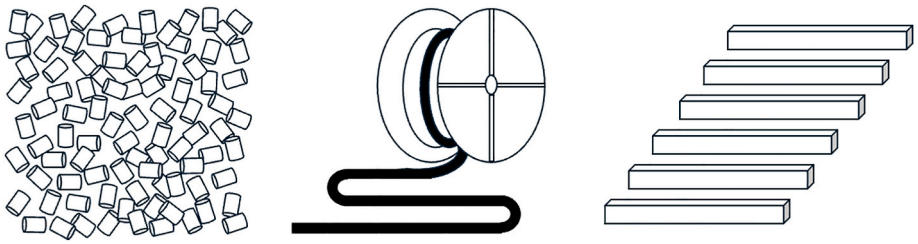

Fig. 2. Illustration of the granulate, filament and 3D-printed specimens.

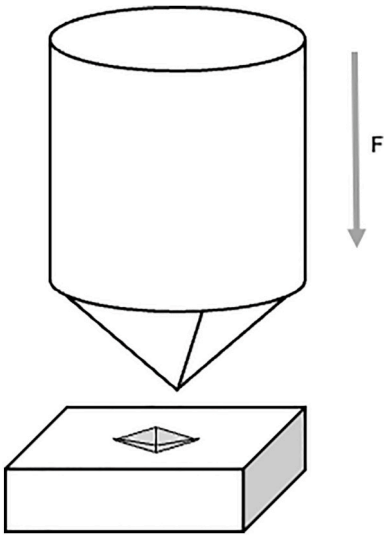

Fig. 3. Set-up for the measurement of the Martens parameters.

ZwickRoell).

2.5. Flexural strength measurement

For FS measurement, the final dimension of each specimen was determined using a digital micrometer (Mitutoyo IP65, Mitutoyo Corporation, Kawasaki, Japan) with an accuracy of ±0.05 mm. Three-point FS was tested in a universal testing machine (Zwick 1445, ZwickRoell) set at a crosshead speed of 1 mm/min (Fig. 4). FS was calculated using the following formula: $\sigma = 3Pl/(2\ wb^2)$ (Technical Committee ISO, 2011), where σ: flexural strength (MPa), P: ultimate load (N), l: the test span (mm), w: specimen width (mm), b: specimen thickness (mm).

2.6. Shear bond strength measurement

SBS was determined in a universal testing machine (Zwick 1445, ZwickRoell) with a crosshead speed of 0.5 mm/min. Specimens were axially adjusted to the loading direction of the testing machine using a special testing fixture that allowed a torque-free axial force application. The load until failure was measured and SBS was calculated using the

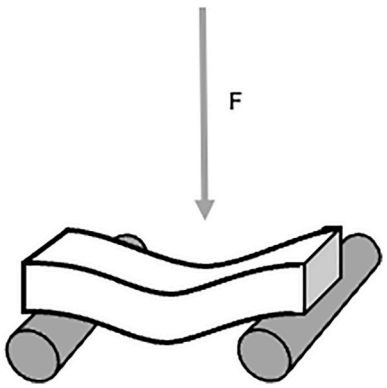

Fig. 4. Set-up for the measurement of the flexural strength.

following equation: SBS = F/A (MPa) (Technical Committee ISO, 2011), where F is the force at failure [N] and A is the bonding area [mm^2].

2.7. Leaching tests

For the leaching tests, specimens with a weight of 42 mg were cut and put into 19 ml 5 vol.-% HNO_3 tempered at 55 °C. The silver content of the liquid was analyzed by atomic absorption spectroscopy (Aanalyst 400, Silver (328.07 nm) PerkinElmer, Waltham, USA) after 1-, 3-, 7-, 14-, 21-, 28- and 42 days.

2.8. Statistical analysis

Data were descriptively analyzed and the normality of the data distribution was tested using the Kolmogorov–Smirnov test. The effect of the different variables on the Martens parameters was examined with two-way ANOVA. Significant differences between groups were analyzed with the Kruskal–Wallis and Mann–Whitney *U* test. FS and SBS were analyzed using two-way ANOVA and unpaired t-tests. The Weibull modulus was calculated using the maximum likelihood estimation method at a 95% confidence level (Butikofer et al., 2015). Fracture types were classified, and relative frequencies computed using the Ciba-Geigy table. The significance level was defined at $p < 0.05$ for all statistical tests. The analyses were conducted using the IBM SPSS Statistics 29.0 Software (IBM, Amonk, USA).

3. Results

3.1. SEM images and EDX mappings

While the unfilled PPSU specimens presented a smooth surface structure, the filled PPSU2-GR showed small mounds that could represent the zeolite fillers (Fig. 5).

PPSU2-FI displayed an inhomogeneous surface characterized by micro pits. These micro pits seemed to fuse together and dissolve or persist as smaller micro pits in the processed PPSU2-3D. In PPSU1-3D and PPSU2-3D, the print layers can be clearly distinguished.

The silicon atoms present in the zeolite lattice are depicted as red points. A homogeneous distribution of the zeolite within the filled PPSU was observed for all three processing steps.

3.2. Martens parameters

As 40% of the HM and 73% of the E_{IT} groups showed a deviation from the normal distribution, non-parametric tests were computed. The PPSU material showed the highest impact on the Martens parameters (HM: partial eta squared (η_p^2) = 0.959, $p < 0.001$; E_{IT}: $\eta_p^2 = 0.964$, $p < 0.001$), followed by the interaction between the PPSU material and the aging level (HM: $\eta_p^2 = 0.103$, $p < 0.001$; E_{IT}: $\eta_p^2 = 0.111$, $p < 0.001$) and the aging level (HM: $\eta_p^2 = 0.097$, $p < 0.001$; E_{IT}: $\eta_p^2 = 0.106$, $p < 0.001$). As the interaction between the two parameters was found to be significant, data were split, and separate analyses were performed for each parameter.

PPSU1-GR specimens aged 10,000 TC + 36 d + 10,000 TC showed lower Martens parameters than observed initially (HM: $p < 0.001$; E_{IT}: $p = 0.015$) and a lower HM than reported for specimens aged 10,000 TC +

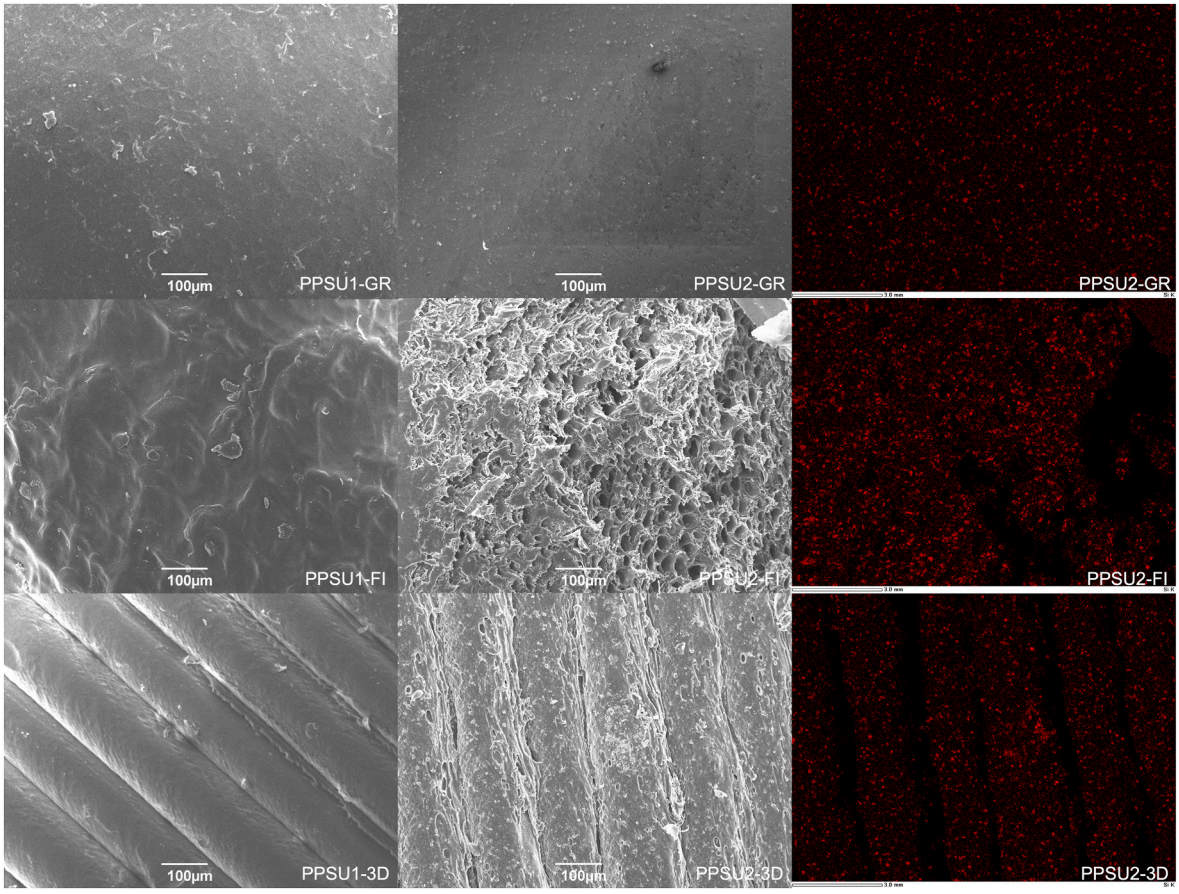

Fig. 5. SEM images (left) and silicon mapping analyses by EDX (right) for the different groups at a x150 magnification (PPSU1 – unfilled, PPSU2 – filled; GR – granulate, FI – filament, 3D – 3D-printed). Silicon atoms are shown in red.

36 d ($p = 0.036$) (Tables 2 and 3). In addition, initially measured specimens presented a higher HM compared to specimens aged with 5000 TC ($p = 0.009$).

For PPSU1-FI, initial HM values were higher than those observed after aging ($p < 0.001$). Initial specimens furthermore showed a higher E_{IT} than specimens aged with 10,000 TC + 36 d ($p < 0.001$) and 10,000 TC + 36 d + 10,000 TC ($p < 0.001$).

Within 3D-printed PPSU1 specimens, aging with 10,000 TC + 36 d + 10,000 TC led to lower HM values than observed for the other aging levels ($p < 0.001$–0.031). An exception is the group aged with 10,000 TC, that reported values in the same range as observed after 10,000 TC + 36 d + 10,000 TC ($p = 0.206$). With respect to the E_{IT}, aging with 10,000 TC + 36 d + 10,000 TC resulted in lower values than observed after 10,000 TC + 36 d ($p = 0.041$).

For all filled PPSU groups (PPSU2-GR: HM: $p = 0.611$ & E_{IT}: $p = 0.395$; PPSU2-FI: HM: $p = 0.780$ & E_{IT}: $p = 0.561$; PPSU2-3D: HM: $p = 0.053$ & E_{IT}: $p = 0.191$), no impact of the aging level on the Martens parameters was observed.

The highest HM and E_{IT} values were observed for PPSU1-GR and PPSU1-FI, followed by PPSU2-GR and PPSU1-3D ($p < 0.001$). The lowest HM and E_{IT} values were reported for PPSU2-FI, followed by PPSU2-3D ($p < 0.001$), regardless of the aging level.

3.3. Flexural strength

The Kolmogorov-Smirnov test indicated no violation of the assumption of normality, which is close to the primary error for a statistical test. Therefore, the assumption of normal distribution was used. The PPSU filament ($\eta_p^2 = 0.848$, $p < 0.001$) showed the highest impact on FS. The interaction (PPSU filament versus aging level) was also significant ($\eta_p^2 = 0.147$, $p < 0.001$). As the higher order interactions were found to be significant, the fixed effects of PPSU filament and aging level could not be compared directly. Consequently, several different analyses were computed and divided by the levels of PPSU filament and aging level depending on the hypothesis of interest (Table 4).

Within PPSU1-3D, initially tested specimens showed lower FS values compared to specimens aged with 10,000 TC ($p = 0.025$). Within PPSU2-3D, initial specimens presented higher FS results than observed after aging ($p = 0.001$). For both PPSU materials, aged specimens showed higher Weibull module than reported initially.

Unfilled PPSU1-3D showed higher FS than filled PPSU2-3D ($p < 0.001$). The Weibull module of the two PPSU materials were observed to be in the same value range.

3.4. Shear bond strength

No violation of the assumption of normality was found and therefore the data was analyzed with the assumption of normal distribution. The adhesive system showed the highest impact on the SBS values ($\eta_p^2 = 0.509$, $p < 0.001$), followed by the resin composite ($\eta_p^2 = 0.072$, $p = 0.042$). Furthermore, the interaction (adhesive system versus resin composite) was significant ($\eta_p^2 = 0.589$, $p < 0.001$). Therefore, the fixed effects of adhesive system and resin composite could not be compared directly, and several different analyses were computed and divided by levels of adhesive system and resin composite depending on the hypothesis of interest (Table 5).

Using the adhesive system PR resulted in no bonding between PPSU and the veneering resin composite. Higher SBS values to the veneering resin composite were observed for SB than for CQ ($p < 0.001$).

For the luting resin composite, no differences in bond strength were detected between the different adhesive systems ($p = 0.059$).

Adhesive fractures between PPSU2-3D and the adhesive system occurred most frequently, followed by mixed fractures between PPSU2-3D/resin composite and the adhesive system (Table 6). Adhesive fractures between the resin composite and the adhesive system only occurred for PB.

AD, OC, SB and VL showed higher bond strength in combination with the veneering resin composite than with the luting resin composite. In contrast, PR bonded better to the luting resin composite.

3.5. Leaching behavior

For all three processing steps, a continuous release of silver from the filled PPSU samples was observed over a period of 42 days (Fig. 6).

Except for the measurements after 21 and 28 days, where PPSU2-GR showed an increase in ion release and surpassed PPSU2-FI, PPSU2-GR released the least amount of silver. After 21 and 28 days, PPSU2-FI presented the lowest amount of silver in the solution. PPSU2-3D released the highest amount of silver for all measurement points except day 1, where PPSU2-FI showed the highest leaching. Over the entire duration of the experiment, PPSU2-3D released the highest amount of silver, which corresponds to a release of 9.6% of the silver present in the sample. PPSU2-FI released 4.9% and PPSU2-GR 4.5% of the present amount of silver.

4. Discussion

The purpose of this investigation was to examine the chemical and mechanical properties of PPSU depending on its composition and manufacturing process.

The null hypotheses that (1) the material composition would not show an impact of the surface characteristics of PPSU and (2) that neither the material composition nor (3) aging would show an impact on the Martens parameters and FS were rejected. Unfilled PPSU specimens

Table 2
Descriptive statistics for the HM [N/mm^2].

	PPSU1-GR		PPSU1-FI		PPSU1-3D		PPSU2-GR		PPSU2-FI		PPSU2-3D	
	Mean ± SD	95% CI	Mean ± SD	95% CI	Mean ± SD	95% CI	Mean ± SD	95% CI	Mean ± SD	95% CI	Mean ± SD	95% CI
Initial	116 ± 1.35^{c,D}	114; 117	116 ± 2.59^{ab,D}	113; 118	110 ± 2.98^{ab,C}	108; 112	111 ± 5.23^{a,C}	107; 114	46.0 ± 2.36^{a,A}	43; 48	76.9 ± 7.46^{a,B}	70; 83
5000 TC	112 ± 5.79^{aab,C}	108; 115	111 ± 2.68^{aa,C}	108; 112	108 ± 3.19^{ab,C}	105; 110	108 ± 5.86^{a,C}	104; 112	43.9 ± 1.85^{aa,A}	41; 46	68.0 ± 9.59^{a,B}	60; 75
10,000 TC	113 ± 3.34^{aabc,D}	110; 115	111 ± 1.64^{aa,CD}	109; 112	107 ± 4.07^{aab,C}	103; 109	110 ± 3.80^{a,CD}	107; 112	45.1 ± 3.87^{a,A}	41; 48	73.2 ± 7.51^{a,B}	66; 79
10,000 TC + 36 d	113 ± 2.25^{abc,C}	111; 115	110 ± 3.45^{a,C}	107; 112	108 ± 5.00^{b,C}	104; 111	110 ± 6.85^{a,C}	105; 114	44.8 ± 2.66^{aa,A}	41; 47	76.8 ± 6.80^{a,B}	70; 82
10,000 TC + 36 d + 10,000 TC	110 ± 3.93^{aa,D}	106; 112	109 ± 2.12^{a,CD}	106; 110	103 ± 6.39^{aa,C}	99.0; 107	110 ± 3.94^{a,D}	107; 113	44.9 ± 5.76^{aa,A}	39; 50	76.8 ± 6.80^{a,B}	70; 82

ab Different letters present significant differences between aging levels within one PPSU material.
AB Different letters present significant differences between PPSU materials within one aging level.
[a] Not normally distributed.

Table 3
Descriptive statistics for the E_{IT} [N/mm].

	PPSU1-GR		PPSU1-FI		PPSU1-3D		PPSU2-GR		PPSU2-FI		PPSU2-3D	
	Mean ± SD	95% CI	Mean ± SD	95% CI	Mean ± SD	95% CI	Mean ± SD	95% CI	Mean ± SD	95% CI	Mean ± SD	95% CI
Initial	2.76 ± 0.08^{a,b,CD}	2.6; 2.8	2.82 ± 0.05^{a,c,D}	2.6; 2.9	2.59 ± 0.04^{a,ab,C}	2.4; 2.7	2.77 ± 0.22^{a,a,CD}	2.5; 2.9	1.73 ± 0.33^{a,a,A}	1.3; 2.0	2.21 ± 0.20^{a,B}	1.9; 2.4
5000 TC	2.66 ± 0.28^{a,ab,C}	2.4; 2.8	2.74 ± 0.08^{a,bc,C}	2.6; 2.8	2.57 ± 0.05^{a,ab,C}	2.4; 2.6	2.71 ± 0.28^{a,C}	2.4; 2.9	1.60 ± 0.07^{a,a,A}	1.4; 1.7	2.04 ± 0.16^{a,B}	1.8; 2.2
10,000 TC	2.73 ± 0.19^{a,ab,CD}	2.5; 2.9	2.74 ± 0.06^{a,bc,CD}	2.6; 2.8	2.57 ± 0.05^{a,ab,C}	2.4; 2.6	2.85 ± 0.18^{a,D}	2.6; 3.0	1.65 ± 0.14^{a,A}	1.4; 1.8	2.15 ± 0.18^{a,B}	1.9; 2.3
10,000 TC + 36 d	2.71 ± 0.11^{a,ab,CD}	2.5; 2.8	2.65 ± 0.12^{a,CD}	2.4; 2.8	2.61 ± 0.09^{a,b,C}	2.4; 2.7	2.80 ± 0.23^{a,a,D}	2.5; 3.0	1.60 ± 0.11^{a,A}	1.4; 1.7	2.18 ± 0.13^{a,a,B}	1.9; 2.3
10,000 TC + 36 d + 10,000 TC	2.56 ± 0.18^{a,a,C}	2.3; 2.7	2.69 ± 0.10^{a,ab,CD}	2.5; 2.8	2.54 ± 0.09^{a,a,C}	2.3; 2.6	2.79 ± 0.20^{a,D}	2.5; 2.9	1.65 ± 0.20^{a,a,A}	1.3; 1.9	2.18 ± 0.13^{a,a,B}	1.9; 2.3

ab Different letters present significant differences between aging levels within one PPSU material.
AB Different letters present significant differences between PPSU materials within one aging level.
[a] Not normally distributed.

Table 4
Descriptive statistics for the three-point flexural strength values of PPSU1-3D and PPSU2-3D [MPa].

	PPSU1-3D			PPSU2-3D		
	Mean ± SD	95% CI	Weibull module (95 % CI)	Mean ± SD	95% CI	Weibull module (95 % CI)
Initial	138 ± 20^{a,B}	127; 147	8.1 (5.0; 12.8)^{a,A}	102 ± 11^{b,A}	93; 110	12 (6.0; 21)^{a,A}
5000 TC	146 ± 6^{ab,B}	141; 149	30 (19; 48)^{b,A}	94 ± 5^{a,A}	90; 97	22 (13; 35)^{b,A}
10,000 TC	148 ± 7^{b,B}	144; 152	27 (15; 43)^{b,A}	92 ± 5^{a,A}	88; 94	22 (13; 35)^{b,A}

ab Different letters present significant differences between aging levels within one PPSU material.
AB Different letters present significant differences between PPSU materials within one aging level.
* Not normally distributed.

Table 5
Descriptive statistics for the SBS of PPSU2-3D to the veneering and luting resin composite using different adhesive systems [MPa].

	Veneering resin composite		p-values for the differences between the two resin composites	Luting resin composite	
	Mean ± SD	95% CI		Mean ± SD	95% CI
AD	21.2 ± 4.6^{bc,B}	14; 27	**0.041**	15.2 ± 2.1^{a,A}	11; 18
CQ	11.8 ± 3.7^{b,A}	6; 17	0.212	15.4 ± 4.8^{a,A}	8; 22
OC	17.8 ± 3.8^{bc,B}	12; 23	**0.035**	11.7 ± 3.9^{a,A}	5; 17
PB	12.8 ± 3.9^{bc,A}	6; 18	0.058	7.0 ± 4.3^{a,A}	1; 13
PR	0 ^{a,A}	–	<**0.001**	16.2 ± 2.0^{a,B}	12; 19
SB	22.2 ± 6.0^{c,B}	13; 30	**0.033**	12.5 ± 6.0^{a,A}	4; 20
VL	19.5 ± 2.5^{bc,B}	15; 23	**0.004**	13.7 ± 2.0^{a,A}	10; 17

ab Different letters present significant differences between adhesive systems within one resin composite.
AB Different letters present significant differences between resin composites within one adhesive system.
[a] Not normally distributed.

presented a homogenous surface and high Martens parameters, with PPSU1-GR and PPSU1-FI showing the highest HM and E_{IT} values. As no consistent difference in performance could be discerned between the unfilled granulate and filament, this processing step does not seem to harm the mechanical properties of PPSU. Processing by 3D-printing led to similar or slightly lower results. While a previous investigation reported significantly lower FS values for 3D-printed PPSU specimens in comparison with injection molded counterparts of the same composition and called for a reevaluation and optimization of the additive manufacturing strategy (Schonhoff et al., 2021), the present results indicate the employed printing parameters to be well defined for unfilled PPSU. This finding matches the recent advances made for 3D-printed PEEK (Li and Lou, 2020).

Although high-performance thermoplastics are valued for their low solubility and water absorption (Liebermann et al., 2016), a decrease in Martens parameters has previously been reported for 3D-printed and milled polyaryletherketone materials after aging (Prechtel et al., 2020). The maximum aging period of 10,000 TC + 36 d + 10,000 TC employed in this investigation is estimated to be equivalent to approximately 2 years in vivo (Gale and Darvell, 1999). While aging led to reduced Martens parameters in unfilled PPSU, the FS and Weibull modulus increased. The repetitive change in ambient temperature and constant exposure to water during thermocycling may impair the PPSU specimens' surface properties that were quantified by a decrease in Martens parameters. On the other hand, artificial aging could encourage the fusion of the different print layers and initiate stress relief within a specimen that entails an increase in its mechanical properties. Internal stress relief could furthermore translate into a more homogenous fault distribution, as perceived in the increased Weibull module. A previous investigation examining three different PPSU materials reported no impact and both a positive and a negative influence of aging on FS (Schonhoff et al., 2021). Further studies are warranted to investigate the aging properties of PPSU more closely.

Interestingly, the observations made for the unfilled PPSU groups did not transfer to their zeolite filled counterparts. Within these groups, the filament showed the lowest Martens parameters. The processing from granulate to filament thus seems to exercise a negative impact on the properties of filled PPSU. This observation is illustrated in the SEM images: after extrusion from the granulate, micro pits are clearly visible in the filament. Additional processing by additive manufacturing then again led to higher Martens parameters than observed for the filament. In the 3D-printed specimen, the micro pits seem to fuse together and dissolve or persist as smaller pits. In line with the observed Martens parameters, filled PPSU2-3D presented lower FS results than seen for the unfilled PPSU1-3D. However, as similar Martens parameters were reported for the filled granulate and the unfilled PPSU groups, the observed difference between the 3D-printed materials in regard to both

Table 6
Relative frequencies of fracture types with 95% Confidence Intervals for the SBS of PPSU2-3D to the veneering and luting resin composite using different adhesive systems.

	Veneering resin composite			Luting resin composite		
	Adhesive fracture between PPSU2-3D and adhesive system	Mixed fracture between PPSU2-3D/resin composite and adhesive system	Adhesive fracture between resin composite and adhesive system	Adhesive fracture between PPSU2-3D and adhesive system	Mixed fracture between PPSU2-3D/resin composite and adhesive system	Adhesive fracture between resin composite and adhesive system
AD	100 [46; 100]	0 [0; 53]	0 [0; 53]	100 [46; 100]	0 [0; 53]	0 [0; 53]
CQ	60 [13; 95]	40 [4; 86]	0 [0; 53]	100 [46; 100]	0 [0; 53]	0 [0; 53]
OC	80 [27; 100]	20 [0; 72]	0 [0; 53]	80 [27; 100]	20 [0; 72]	0 [0; 53]
PB	0 [0; 53]	40 [4; 86]	60 [13; 95]	0 [0; 53]	40 [4; 86]	60 [13; 95]
PR	0 [0; 53]	100 [46; 100]	0 [0; 53]	100 [46; 100]	0 [0; 53]	0 [0; 53]
SB	100 [46; 100]	0 [0; 53]	0 [0; 53]	80 [27; 100]	20 [0; 72]	0 [0; 53]
VL	20 [0; 72]	80 [27; 100]	0 [0; 53]	80 [27; 100]	20 [0; 72]	0 [0; 53]

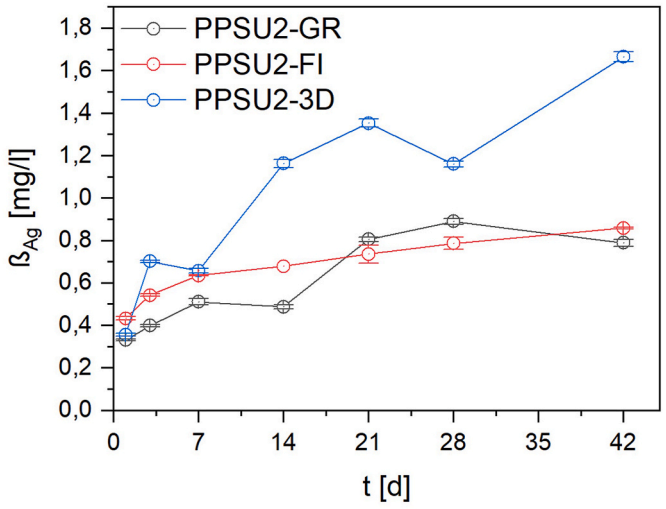

Fig. 6. Leaching behavior of filled PPSU (GR – granulate, FI – filament, 3D – 3D-printed).

their Martens parameters as well as their FS may not be caused by their composition but an insufficient adaptation of the processing parameters to the filled PPSU material. Filled PPSU specimens were printed with the Apium P220, a successor of the Apium P155, that possesses a larger printing volume. Specimens were processed with a 10 °C reduced zone heating and a 50% higher printing speed of 600 mm/min. Although these changes constitute substantial time savings, they should be critically evaluated as the mechanical properties of the printed objects may suffer. While first studies report promising findings for the processing of filled polymers by fused filament fabrication (Spoerk et al., 2017; Vidakis et al., 2021), a filler percentage as low as 4.0 wt% is viewed as a potential threshold due to processability challenges (Vidakis et al., 2021). To the authors' best knowledge, this is the first investigation that examined a filled PPSU composition. Additional research aiming to optimize the processing parameters, both during extrusion from granulate and during 3D-printing from filament, are warranted in this seminal field.

While the Martens parameters of filled PPSU were no affected by aging, the FS decreased. For resin composites, a loosening of filler particles during aging that later on impairs the mechanical properties of said materials has been reported (Oja et al., 2021). A loosening of the zeolite fillers may thus explain the reduced FS values reported after aging. Further research is warranted to investigate why the Martens parameters of filled PPSU were not affected by this process and focus on the surface morphology of filled PPSU after extended aging regimens. Remarkably, the Weibull module of filled PPSU were higher for aged specimens. In this context, aging may have equalized differences that were previously present between high- and low-end performing specimens.

The null hypothesis that (4) the adhesive systems would not influence the SBS to a veneering resin composite was rejected, while the null hypothesis concerning the luting resin composite was accepted, with the adhesive system not showing an impact on the adhesion to the luting resin composite. With adhesive fractures between PPSU2-3D and the adhesive system being predominant, this junction represented the weakest link. With the observed values for the luting resin composite ranging between 7.0 and 16.2 MPa, it may, however, be concluded that the different adhesive systems are in conjunction with the employed luting resin composite equally suited to successfully fix a prosthetic restoration 3D-printed from filled PPSU. The absence of differences between the different conditioning procedures could also indicate that this pretreatment step may play a minor role in comparison to the preceding air-particle abrasion with aluminum-oxide particles (Mayinger et al., 2021). The employed abrasion parameters were based on the findings of a previous investigation that reported an increased surface free energy and surface roughness following an increase in pressure and particle size (Schonhoff et al., 2022).

Interestingly, the choice of adhesive system affected the SBS to the veneering resin composite. Here, a conditioning with PR did not entail a successful adhesion. This may either be caused by the composition of the adhesive system, or its application and processing. As the manufacturing guidelines detailing the duration of the massaging in, the blowing off and the polymerization of the adhesive system did not differ from those employed for the superiorly performing OC or SB, PR's composition must constitute the decisive factor. As the manufactures do not provide the exact chemical configuration of their adhesive systems, a sound comparison between materials is challenging. The determination of the contact angle between the different adhesives and the PPSU substrate could enhance our knowledge about the wettability of the tested systems. In theory, a low viscosity and ensuing higher wettability should entail an improved adhesion. Other factors that should be considered when regarding the performance of universal adhesives include their degree of conversion and associated mechanical properties, and the composition of their functional groups that bond with the substrate. On the basis of the present findings, the use of the adhesive system PR cannot be recommended for conditioning prior to the veneering of PPSU. When regarding the other adhesive systems, SBS values of 11.8–22.2 MPa were observed. The slightly poorer performance of CQ must once again be connected to its chemical composition. To guarantee a high adhesion between PPSU and veneering resin composite, the use of all tested adhesive systems except for PR and CQ is thus suggested. In view of the differing manufacturing guidelines employed for the similarly performing adhesive systems AD, OC, PB, SB and VL, the processing procedures and choice of polymerization device may be negligible in the face of their varying chemical compositions.

Except for PR, the observed SBS values were higher for the veneering than the luting resin composite. While the veneering resin composite is refined with inorganic fillers, the luting resin composite is characterized by the addition of triethylene glycol dimethacrylate that ensures its

required higher flowability.

The present results for the successful esthetic veneering and luting of 3D-printed filled PPSU are underlined by two landmark investigations examining unfilled PPSU that have previously reported sufficient tensile bond strength to a veneering resin composite and promising fracture load values for manually veneered single-unit FDPs (Schonhoff et al., 2022; Mayinger et al., 2023). Additional studies are warranted to confirm the present findings and determine the long-term behavior of filled PPSU restorations in a clinically relevant set-up.

The null hypotheses that (5) neither the material composition nor (6) the progression of release time would present an influence on the leaching properties of PPSU were rejected. 3D-printed objects showed the highest release of silver ions, with all compositions dispensing silver over the examined period of 42 days. As silver coated zeolites were incorporated into the molten PPSU, silver ions were available on the inner and outer surface of the thermoplastic. It can be assumed that at first the silver is released from zeolites near the surface. Over time, the silver from deeper zeolite layers will be dispensed. Previous studies have shown the antimicrobial effect of acrylic resins doted with silver incorporating zeolites against bacterial strains such as *s. mutans*, *f. nucleatum* and *c. albicans* (Boschetto et al., 2012; Kuroki et al., 2010; Malic et al., 2019; Stencel et al., 2018; Yamamoto et al., 1996; Wakweya and Jifar, 2023; Cometa et al., 2022). A systematic review underlined the potential of ion-incorporated zeolites in enhancing the antimicrobial properties of dental materials, although the mechanical properties of some materials, such as MTA and acrylic resin, which depend on the zeolite concentration, may be compromised (Hao et al., 2021). In the conclusion, adding 0.2-2 wt% zeolite was suggested (Hao et al., 2021). The successful homogenous doping of PPSU in the present investigation, either in its granulate, filament or 3D-printed form, is clearly visualized in the EDX images. The differences in the release of silver between the three processing forms can be attributed to the varying surface/volume ratio, with 3D-printed molded objects possessing gaps and voids between the printing lanes, which are probably caused by an under extrusion during the printing process, that increase the contact surface for the silver ion release. While the partially observed differences between the filament and granulate seem negligible, future studies should investigate why the granulate showed an increased silver ion release after 14 days surpassing that observed for the filament.

The results of the present investigation must be evaluated in regard to their limitations. As silver ions have been observed to show bactericidal and cytotoxic properties (Liao et al., 2019), future investigations should encompass biocompatibility testing. The determination of the surface free energy and surface roughness and the inclusion of a negative control group (no adhesive system) in the evaluation of the reported SBS values and a positive control group (e.g., PEEK or acrylic resin) as an alternative to the different PPSU compositions would increase the validity of the reported findings. In addition, a variation of the processing parameters of the filament (inter alia: pre-drying of the granulate, pressure during extrusion) and the 3D-printed object (inter alia: printing speed and strategy, printing temperatures) for both unfilled and filled PPSU compositions and an evaluation of the resulting material properties is warranted to define an ideal workflow. To confirm the trends observed in the present investigation in a clinical setting, long-term clinical studies are necessary.

5. Conclusion

This investigation provides proof of principle that the thermoplastic PPSU can be successfully doped with silver coated zeolite fillers. A silver ion release could be observed for a period of 6 weeks, with the analysis of the leaching behavior revealing that 3D-printed objects dispensed the highest amount of silver. The evaluation of the SBS between PPSU and a veneering or luting resin composite following conditioning with different adhesive systems confirmed the feasibility of esthetically veneering and luting filled PPSU restorations. To achieve mechanical properties similar to those reported for unfilled PPSU, the processing parameters of filled PPSU require further refinement.

Funding

This work was supported by research program ZF4052006AW8 (AiF Projekt GmbH, Berlin, Germany, ZIM-Kooperationsprojekte, Projektträger des BMWi).

CRediT authorship contribution statement

Felicitas Mayinger: Writing – review & editing, Writing – original draft, Visualization, Formal analysis. **Andrea Lösch:** Writing – review & editing, Investigation, Formal analysis. **Elena Reznikova:** Writing – review & editing, Investigation. **Christian Wilhelm:** Writing – review & editing, Methodology, Conceptualization. **Bogna Stawarczyk:** Writing – review & editing, Project administration, Methodology, Funding acquisition, Formal analysis, Conceptualization.

Declaration of competing interest

The authors declare that they have no known competing financial interests or personal relationships that could have appeared to influence the work reported in this paper.

Data availability

Data will be made available on request.

Acknowledgements

The authors would like to thank Lisa Marie Schönhoff and Marlis Eichberger.

References

Boschetto, D.L., Lerin, L., Cansian, R., Pergher, S.B.C., Di Luccio, M., 2012. Preparation and antimicrobial activity of polyethylene composite films with silver exchanged zeolite-Y. Chem. Eng. J. l 204–206, 210–216. https://doi.org/10.1016/j.cej.2012.07.111.

Butikofer, L., Stawarczyk, B., Roos, M., 2015. Two regression methods for estimation of a two-parameter Weibull distribution for reliability of dental materials. Dent. Mater. 31 (2), e33–e50. https://doi.org/10.1016/j.dental.2014.11.014.

Chernousova, S., Epple, M., 2013. Silver as antibacterial agent: ion, nanoparticle, and metal. Angew. Chem., Int. Ed. Engl. 52 (6), 1636–1653. https://doi.org/10.1002/anie.201205923.

Cometa, S., Bonifacio, M.A., Bellissimo, A., Pinto, L., Petrella, A., De Vietro, N., Iannaccone, G., Baruzzi, F., De Giglio, E., 2022. A green approach to develop zeolite-thymol antimicrobial composites: analytical characterization and antimicrobial activity evaluation. Heliyon 8 (5), e09551. https://doi.org/10.1016/j.heliyon.2022.e09551.

Dorf, T., Perkowska, K., Janiszewska, M., Ferrer, I., Ciurana, J., 2018. Effect of the main process parameters on the mechanical strength of polyphenylsulfone (PPSU) in ultrasonic micro-moulding process. Ultrason. Sonochem. 46, 46–58. https://doi.org/10.1016/j.ultsonch.2018.03.024.

Fountas, N.A., Papantoniou, I., Kechagias, J.D., Manolakos, D.E., Vaxevanidis, N.M., 2022. Modeling and optimization of flexural properties of FDM-processed PET-G specimens using RSM and GWO algorithm. Eng. Fail. Anal. 138, 106340. https://doi.org/10.1016/j.engfailanal.2022.106340.

Gale, M.S., Darvell, B.W., 1999. Thermal cycling procedures for laboratory testing of dental restorations. J. Dent. 27 (2), 89–99. https://doi.org/10.1016/s0300-5712(98)00037-2.

Hao, J., Lang, S., Mante, F., Pavelic, K., Ozer, F., 2021. Antimicrobial and mechanical effects of zeolite use in dental materials: a systematic review. Acta Stomatol. Croat. 55 (1), 76–89. https://doi.org/10.15644/asc55/1/9.

Kechagias, J.D., 2024. Surface roughness assessment of ABS and PLA filament 3D printing parts: structural parameters experimentation and semi-empirical modelling. Int. J. Adv. Manuf. Technol. 134, 1935–1946. https://doi.org/10.1007/s00170-024-14232-0.

Kuroki, K., Hayashi, T., Sato, K., Asai, T., Okano, M., Kominami, Y., Takahashi, Y., Kawai, T., 2010. Effect of self-cured acrylic resin added with an inorganic antibacterial agent on Streptococcus mutans. Dent. Mater. J. 29 (3), 277–285. https://doi.org/10.4012/dmj.2009-076.

Li, Y., Lou, Y., 2020. Tensile and bending strength improvements in PEEK parts using fused deposition modelling 3D printing considering multi-factor coupling. Polymers 12 (11), 2497. https://doi.org/10.3390/polym12112497.

Liao, C.C., Li, Y., Tjong, S.C., 2019. Bactericidal and cytotoxic properties of silver nanoparticles. Int. J. Mol. Sci. 20 (2), 449. https://doi.org/10.3390/ijms20020449.

Liaw, C.Y., Tolbert, J.W., Chow, L.W., Guvendiren, M., 2021. Interlayer bonding strength of 3D printed PEEK specimens, Soft. Matter 17 (18), 4775–4789. https://doi.org/10.1039/d1sm00417d.

Liebermann, A., Wimmer, T., Schmidlin, P.R., Scherer, H., Loffler, P., Roos, M., Stawarczyk, B., 2016. Physicomechanical characterization of polyetheretherketone and current esthetic dental CAD/CAM polymers after aging in different storage media. J. Prosthet. Dent 115 (3), 321–328 e2. https://doi.org/10.1016/j.prosdent.2015.09.004.

Malic, S., Rai, S., Redfern, J., Pritchett, J., Liauw, C.M., Verran, J., Tosheva, L., 2019. Zeolite-embedded silver extends antimicrobial activity of dental acrylics. Colloids Surf. B Biointerfaces 173, 52–57. https://doi.org/10.1016/j.colsurfb.2018.09.043.

Mayinger, F., Fiebig, M., Roos, M., Eichberger, M., Lumkemann, N., Stawarczyk, B., 2021. Bonding behavior between polyetheretherketone and polymethylmethacrylate acrylic denture polymer. J. Adhesive Dent. 23 (2), 145–158. https://doi.org/10.3290/j.jad.b1079579.

Mayinger, F., Eichberger, M., Schonhoff, L.M., Stawarczyk, B., 2023. Fracture load of veneered and monolithic single-unit fixed dental prostheses made from the high-performance thermoplastic polyphenylene sulfone. Int. J. Prosthodont. (IJP) 343–353. https://doi.org/10.11607/ijp.7675.

Naveed, N., Anwar, M.N., 2024. Optimising 3D printing parameters through experimental techniques and ANOVA-Based statistical analysis. SPE Polym 5 (2), 228–240. https://doi.org/10.1002/pls2.10122.

Oja, J., Lassila, L., Vallittu, P.K., Garoushi, S., 2021. Effect of accelerated aging on some mechanical properties and wear of different commercial dental resin composites. Materials 14 (11), 2769. https://doi.org/10.3390/ma14112769.

Prechtel, A., Reymus, M., Edelhoff, D., Hickel, R., Stawarczyk, B., 2020. Comparison of various 3D printed and milled PAEK materials: effect of printing direction and artificial aging on Martens parameters. Dent. Mater. 36 (2), 197–209. https://doi.org/10.1016/j.dental.2019.11.017.

Schonhoff, L.M., Mayinger, F., Eichberger, M., Reznikova, E., Stawarczyk, B., 2021. 3D printing of dental restorations: mechanical properties of thermoplastic polymer materials. J. Mech. Behav. Biomed. Mater. 119, 104544. https://doi.org/10.1016/j.jmbbm.2021.104544.

Schonhoff, L.M., Mayinger, F., Eichberger, M., Losch, A., Reznikova, E., Stawarczyk, B., 2022. Three-dimensionally printed and milled polyphenylene sulfone materials in dentistry: tensile bond strength to veneering composite resin and surface properties after different pretreatments. J. Prosthet. Dent 93–99. https://doi.org/10.1016/j.prosdent.2020.12.042.

Spoerk, M., Sapkota, J., Weingrill, G., Fischinger, T., Arbeiter, F., Holzer, C., 2017. Shrinkage and warpage optimization of expanded-perlite-filled polypropylene composites in extrusion-based additive manufacturing. Macromol. Mater. Eng. 302 (10), 1700143. https://doi.org/10.1002/mame.201700143.

Stencel, R., Kasperski, J., Pakiela, W., Mertas, A., Bobela, E., Barszczewska-Rybarek, I., Chladek, G., 2018. Properties of experimental dental composites containing antibacterial silver-releasing filler. Materials 11 (6), 2173. https://doi.org/10.3390/ma11112173.

Technical Committee ISO/TC 106/SC 2, Dentistry — Polymer-Based Crown and Veneering Materials (ISO 10477:2021), 2011. International Organization for Standardization, Geneva.

Technical Committee ISO/TC 106/SC 1, 2015. Dentistry — Testing of Adhesion to Tooth Structure (ISO/TS 11405:2015). International Organization for Standardization, Geneva.

Technical Committee ISO/TC 164/SC 3, 2022. Metallic Materials — Instrumented Indentation Test for Hardness and Materials Parameters (ISO 14577-5:2022). International Organization for Standardization, Geneva.

Vidakis, N., Petousis, M., Velidakis, E., Tzounis, L., Mountakis, N., Kechagias, J., Grammatikos, S., 2021. Optimization of the filler concentration on fused filament fabrication 3D printed polypropylene with titanium dioxide nanocomposites. Materials 14 (11), 3076. https://doi.org/10.3390/ma14113076.

Wakweya, B., Jifar, W.W., 2023. In vitro evaluation of antibacterial activity of synthetic zeolite supported AgZno nanoparticle against a selected group of bacteria. J. Exp. Pharmacol. 15, 139–147. https://doi.org/10.2147/JEP.S396118.

Wang, Y., Muller, W.D., Rumjahn, A., Schmidt, F., Schwitalla, A.D., 2021. Mechanical properties of fused filament fabricated PEEK for biomedical applications depending on additive manufacturing parameters. J. Mech. Behav. Biomed. Mater. 115, 104250. https://doi.org/10.1016/j.jmbbm.2020.104250.

Wenz, L.M., Merritt, K., Brown, S.A., Moet, A., Steffee, A.D., 1990. In vitro biocompatibility of polyetheretherketone and polysulfone composites. J. Biomed. Mater. Res. 24 (2), 207–215. https://doi.org/10.1002/jbm.820240207.

Wickramasinghe, S., Do, T., Tran, P., 2020. FDM-based 3D printing of polymer and associated composite: a review on mechanical properties, defects and treatments. Polymers 12 (7), 1529. https://doi.org/10.3390/polym12071529.

Yamamoto, K., Ohashi, S., Aono, M., Kokubo, T., Yamada, I., Yamauchi, J., 1996. Antibacterial activity of silver ions implanted in SiO2 filler on oral streptococci. Dent. Mater. 12 (4), 227–229. https://doi.org/10.1016/s0109-5641(96)80027-3.

Yang, C., Tian, X., Li, D., Cao, Y., Zhao, F., Shi, C., 2017. Influence of thermal processing conditions in 3D printing on the crystallinity and mechanical properties of PEEK material. J. Mater. Process. Technol. 248, 1–7. https://doi.org/10.1016/J.JMATPROTEC.2017.04.027.